



Share Your Innovations through JACS Directory



Journal of Thin Films Research

Visit Journal at <http://www.jacsdirectory.com/jtfr>

Reproducible Electrodeposition of Hydrogen Molybdenum Bronze Films and Electrochemical Reduction of Carbon Dioxide

Dane W. Scott*, Sami Alharbi

Department of Chemistry, East Tennessee State University, 325 Treasure Lane, Johnson City, TN 37614, United States.

ARTICLE DETAILS

Article history:

Received 15 July 2020

Accepted 06 August 2020

Available online 26 August 2020

Keywords:

Carbon Dioxide

Hydrogen Molybdenum Bronze

Electrodeposition

Electrochemical Reduction

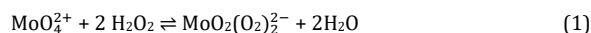
ABSTRACT

Electrochemical synthesis of hydrogen bronze films including molybdenum, tungsten and vanadium are useful electrocatalytic films. This paper describes reproducible hydrogen molybdenum bronze film formation on indium tin oxide and carbon paper substrates by electrodeposition. Film formation is a kinetic process dependent on concentration, time and potential. Bulk electrolysis over time determined the dependence of film thickness on time of deposition. Once the films were prepared, the films were characterized by thickness, conductivity, XPS and X-Ray Diffraction. Cyclic voltammetry in dilute sulfuric acid confirmed that these films are not electrochromic. Hydrogen bronze films on conductive carbon paper were also prepared. Carbon dioxide bubbled into 0.5 M NaHCO₃ using a hydrogen bronze film as the working electrode resulted in formate quantified by ion chromatography. Cyclic voltammetry and Tafel plots using the as deposited films in 0.5 M NaHCO₃ saturated with CO₂ showed catalytic activity toward reduction of carbon dioxide. A Faradaic efficiency of 8% was obtained with an applied potential of -0.4 V.

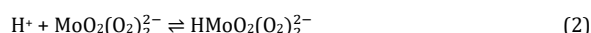
1. Introduction

Over the years, a significant amount of work has been done using hydrogen metal oxide films referred to as hydrogen bronze films. These films have hydrogen incorporated into the oxide. Molybdenum oxide forms a blue hydrogen bronze having the formula H_xMo_x⁵⁺Mo_{1-x}O₃ [1]. Other examples of hydrogen bronze forming oxides include tungsten and vanadium oxide. These films are of interest due to having electrochromic properties, useful as chemical sensors, neutralization of explosives, chemical catalysis and in solar cell technology [2-6]. One potential use for hydrogen bronze films deposited on carbon paper is as an electrocatalyst for reduction of carbon dioxide (CO₂). A number of studies use carbon as a support for electrochemical reduction of CO₂ permitting comparison of proposed research results. Lead and tin alloys on carbon paper have been shown to have high faradaic efficiencies (80%) at -2.0 V vs. Ag/AgCl [7]. Nitrogen doped nanodiamond has been used to reduce CO₂ to acetate with greater than 90% faradaic efficiency requiring an overpotential of -0.8 to -1.0 V vs. RHE [8]. A palladium carbon ink supported on titanium foil has been used for electrochemical reduction. In 0.5 M NaHCO₃ saturated with CO₂ the faradaic efficiency decreases by 80% at -0.35 V in three hours due to carbon monoxide poisoning [9]. Palladium nanoparticles drop-dried on a carbon support is another example in which faradaic efficiency for reduction of CO₂ is 97% with a current density of 22 mA/cm². Once again, after an hour the performance of the catalyst drops quickly due to catalytic poisoning [10]. Just this year, sulfur modified copper catalysts on carbon maintained a faradaic efficiency of up to 80% over 12 hours. However, an over potential of -0.8 V vs. the normal hydrogen electrode (NHE) was required [11]. Nitrogen doped carbon electrocatalysts are gaining attention [12, 13]. Electrochemical reduction experiments resulted in a faradaic efficiency of 93% requiring an over potential of 0.560 V. Performance significantly dropped within the first two hours and retained 63% percent faradaic efficiency after 12 hours [14]. Platinum catalysts have been used to reduce the required overpotential for reducing CO₂ to methane but the faradaic efficiency is only 6.8% [15]. There is a need to continue to develop carbon supported catalyst to reduce the required overpotential for reduction of CO₂ and maintain reduction over long periods of time. This work explores using electrodeposited hydrogen bronze films for reduction of CO₂.

A number of methods result in preparation of hydrogen bronze films. These include metal vapor deposition followed by oxidation, sol-gel methods, thermal decomposition of ammonium heptamolybdate or reacting the oxide with alcohols or glycols [6, 16-19]. One article presses hydrogen molybdenum bronze solid into a pellet exposing one side to sulfuric acid, and silver paste coats the other side. Cyclic voltammetry (CV) in dilute sulfuric acid appears to show reversible intercalation of hydronium ions into the molybdenum oxide lattice. Another method for forming hydrogen bronze films is electrochemical deposition. The film is prepared by deposition on metal substrates or indium tin oxide [20]. Two primary methods involve either dissolution of molybdenum metal or powder in hydrogen peroxide forming peroxytungstate acid which serves as the electrolyte for electrodeposition or dissolving sodium molybdate and adding hydrogen peroxide [2, 21-25]. Co-deposition of the films with platinum is also possible [26]. This article focuses on electrochemical deposition of hydrogen molybdenum bronze due to interest in using the hydrogen bronze film supported on conductive carbon paper as an electrocatalyst. The mechanism by which a blue hydrogen molybdenum bronze can be electrodeposited as a film much like tungsten remains poorly understood [27]. The process of preparing peroxytungstate acid from molybdate and adding hydrogen peroxide is shown below in Eq.(1) [28]:



In doing so, as the reaction proceeds a yellow color results. Continued stirring results in a colorless solution. More peroxide and adjusting to a pH of 2.0 results in the yellow form of peroxytungstate acid shown in Eq. (2) [28]:



This work explores reproducible preparation of hydrogen molybdenum bronze films using molybdate, hydrogen peroxide and sulfuric acid. The resulting solution has been used to electrodeposit hydrogen bronze films onto indium tin oxide(ITO) and conductive carbon substrates. Cyclic voltammetry was used to explore electrochromism of the films. Using carbon dioxide saturated sodium bicarbonate electrolyte and the electrodeposited film as the working electrode, carbon dioxide was reduced to formate quantified by ion chromatography. Cyclic voltammetry showed that the as deposited films are catalytic toward reduction of CO₂. Faradaic efficiency was found to be 8% with an applied potential of -0.4 V.

*Corresponding Author:scottdw@etsu.edu(Dane W. Scott)

2. Experimental Methods

2.1 Materials

All chemicals and conductive carbon sheets were purchased from VWR. The exception was 3% hydrogen peroxide purchased locally. The ITO substrates were purchased from Deposition Research Inc. Ultrapure water was always used and generated using a Millipore system. Airgas provided carbon dioxide. All potentials reported using the silver chloride reference electrode (1.0 M KCl).

2.2 Electrodeposition of Hydrogen Molybdenum Bronze Films

To prepare the peroxymolybdc acid, approximately 2.5 g of sodium molybdate dihydrate was dissolved in 10 mL of 3% hydrogen peroxide. This resulted in yellow solution immediately and a clear solution after stirring overnight. The yellow peroxymolybdc acid solution was generated by adding 10 mL of additional 3% hydrogen peroxide and adjusting the pH to 2.0 using concentrated sulfuric acid dropwise. The solution was used for deposition of hydrogen molybdenum bronze films by bulk electrolysis. A three electrode system was used in which all potentials are reported vs. the silver chloride reference electrode. A platinum wire was used as the counter electrode, and an ITO substrate or conductive carbon square was the working electrode. Bulk electrolysis at -0.4 V electrochemically reduced peroxymolybdc acid to a blue hydrogen bronze film on ITO. Four films using deposition times of 150, 300, 700 and 1400 seconds were prepared.

2.3 Characterization of Films

The four-point probe method was used to measure electrical conductivity of the thin films. Resistance was measured using a Lucas Labs Pro 4-point probe connected to a Keithley 2400 source meter. Film thickness was measured using a Bruker DektakXT® Stylus Profiler. This instrument uses deflection of a cantilever to determine thickness. X-Ray Photoelectron Spectroscopy was performed by Dr. Nicholas Materer also at Oklahoma State University. The XPS measurements were carried out using the Mg anode of a PHI 300W twin anode X-ray source and a PHI double pass cylindrical mirror analyzer having a pass energy of 50 eV. X-Ray Diffraction of films was performed by Dr. Dwight Myers at East Central University using a Bruker D2 Phaser X-Ray diffractometer.

2.4 Electrochemical Reduction of Formate

A hydrogen bronze film prepared by electrodeposition on conductive carbon approximately 3.0 cm² was used in electrochemical reduction of carbon dioxide. The anode cell consisted of the hydrogen bronze film working electrode, a glass pipet to saturate 20 mL of 0.5 M NaHCO₃ with carbon dioxide and the reference. Connecting the anode and cathode was a fritted salt bridge with 0.1 M Na₂SO₄. The cathode consisted of 20 mL 0.5 M NaHCO₃ magnetically stirred and a 2.0 mm diameter platinum wire counter electrode. Carbon dioxide was continuously bubbled without additional stirring for one hour and formate was determined. To understand the kinetics of electrochemical reduction, linear sweep voltammetry was performed from -0.4 to -1.4 V at a scan rate of 4 mV/s.

2.5 Ion Chromatography Quantifying Formate

A 930 Metrohm ion chromatogram using a 20 μL sample loop and Metro Sep A Supp 16-250/4.0 column at 45.0 °C with suppression was used [29]. The eluent was 3.6 mmol Na₂CO₃ at a flow rate of 0.7 mL/minute. Formate has a retention time of 4.6 minutes in 0.5 M NaHCO₃. Peak area of known standards resulted in a calibration for quantifying formate. Carbon dioxide was bubbled into the electrolyte for one hour without an applied potential determine background formate.

3. Results and Discussion

3.1 Film Characterization

3.1.1 Film Thickness

Electrodeposition of the films was carried out at -0.4 V vs. Ag/AgCl reference electrode. Fig. 1 below displays a color photograph of the electrodeposited hydrogen bronze film.



Fig. 1 Hydrogen bronze film after 100 s of electrodeposition on a 1" x 3" ITO slide
<https://doi.org/10.30799/jtrf.025.20040101>

Table 1 Film thickness measurements (μm) of the electrodeposited films versus time

Time (s)	Thickness (μm)	Error (± μm)
100	129	16
300	142	4
700	194	6
1400	462	17

The hydrogen bronze deposited film is dark blue. Table 1 lists film thickness versus time of electrodeposition. As time of deposition increases so does film thickness. One goal was to be able determine how long to deposit films for to obtain a desired thickness as this relationship is not known. Interestingly, the inverse of film thickness decreases versus time and is a linear fit. This plot is shown below in Fig. 2.

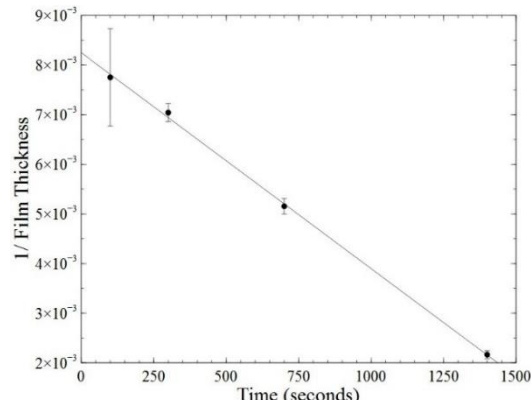


Fig. 2 Plot of film thickness (μm) versus time (s)

Eq.(4) below is the linear fit with an R² value of 0.9995.

$$1/\text{Film Thickness } (\mu\text{m}^{-1}) = -4.4 \times 10^{-6} (\mu\text{m}^{-1}\text{s}^{-1})t + 825.2 (\mu\text{m}^{-1}) \quad (4)$$

One alarming problem with this plot is the error bar at 100 seconds. While the range of film thickness error is 6-17 μm, at lower films thicknesses this results in a much larger error compared to the error of thicknesses measured after 1400 seconds. Nonetheless, within error the plot of the inverse of film thickness with time is linear.

3.1.2 Film Conductivity

One important parameter of an electrocatalytic or photocatalytic film is that the film be conductive. If the film acts as an insulator, this will introduce undesirable impedance to the system or prevent transfer of electrons. Using a 4-point probe, conductivity measurements were obtained. Table 2 below shows the conductivity of the films as function of deposition time.

Table 2 Conductivity of the hydrogen bronze film as a function of deposition time

Time (s)	Conductivity (Ω)	Error (± Ω)
100	3.63	0.03
300	3.81	0.02
700	3.31	0.03
1400	3.58	0.04

While film thickness ranges from 129-462 μm, the sheet resistance is the same in this range. There are two reasons that account for this result. In one situation the four points of the probe reached the ITO substrate. In this case the sheet resistance should match the value of the ITO layered substrate given by the manufacturer, 14 Ω/square. The second possibility is that the electrodeposited sheet film resistance is independent of film thickness. The four point probe measurements result in a sheet resistance less than the ITO layer. This supports the fact that the hydrogen molybdenum bronze films resistance was measured and not the ITO layer.

3.1.3 X-Ray Diffraction

While the XRD of the conductive carbon results in a characteristic peak for carbon paper at 20°, the carbon paper with deposited hydrogen bronze film showed no clear peak and due to being amorphous.

3.1.4 X-Ray Photoelectron Spectroscopy

X-ray photoelectron spectroscopy confirmed that the blue film was composed of molybdenum and oxygen. Peak assignments as assigned in Fig. 3 clearly show that molybdenum is present indicating that electrodeposition results in the blue color due to formation of the blue hydrogen molybdenum bronze.

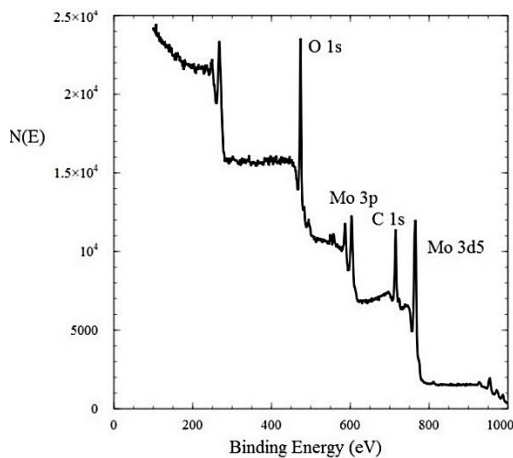


Fig. 3 XRay photoelectron spectroscopy of the electrodeposited film

3.2 Cyclic Voltammetry using of Deposited Films

3.2.1 Electrochromism

A film acting as the working electrode, platinum disc as the counter electrode and reference electrode were utilized to carry out cyclic voltammetry in a negative direction first going from 0 to -0.4 V then +0.4 V. Fig. 4 shows the CV of the film in 0.5 M H₂SO₄ with non-reversible reduction peaks at -0.3 V and -1.2 V. Very quickly, the film disappeared completely indicating dissolution into the bulk of the electrolyte indicating the films are not electrochromic with hydronium ions. There is one article indicating that cathodic current results in mass loss of the due to dissolution into the film, which is consistent with Fig. 4 [30]. The hydrogen molybdenum films are stable under anodic potentials. Electrochemical reduction of carbon dioxide was carried out using these potentials.

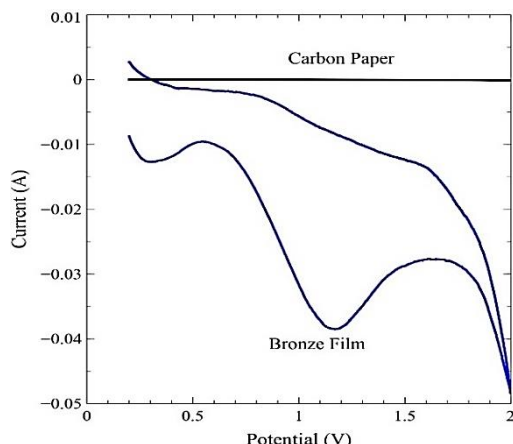


Fig. 4 Cyclic voltammetry of the hydrogen bronze film in 0.5 M sulfuric acid

3.2.2 Evidence for Catalytic Reduction of CO₂

Fig. 5 shows the CV of carbon paper in nitrogen and CO₂ saturated 0.1 M NaHCO₃, while Fig. 6 is the same experiment using electrodeposited films on carbon paper.

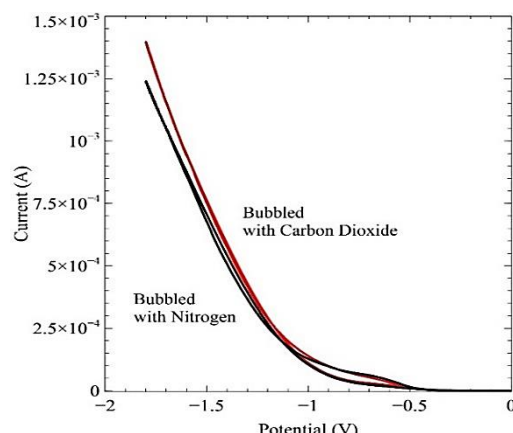


Fig. 5 The CV of carbon paper in nitrogen and CO₂ saturated 0.1 M NaHCO₃ using the silver chloride as a reference electrode
<https://doi.org/10.30799/jtfr.025.20040101>

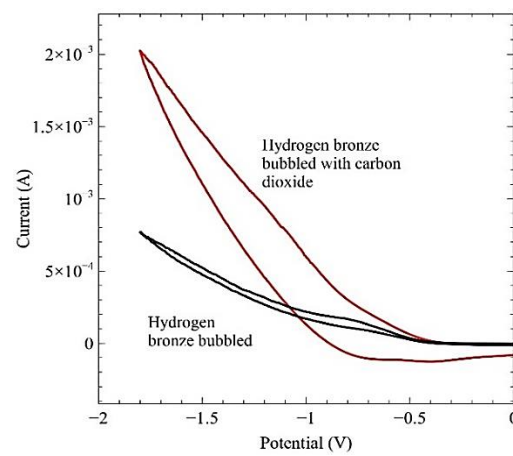


Fig. 6 The CV of carbon paper with the hydrogen molybdenum bronze film in nitrogen and CO₂ saturated 0.1 M NaHCO₃ using the silver chloride as a reference electrode

Fig. 5 shows that there is no increase in current using carbon paper when the electrolyte is saturated with CO₂ compared to that of nitrogen. However, Fig. 6 shows that the onset of reduction of CO₂ starts at an applied potential of -0.4 V. This is evident by an increase in current compared to the CV of carbon paper and hydrogen molybdenum bronze film in nitrogen saturated electrolyte. As such, electrodeposited hydrogen molybdenum bronze films on conductive carbon were used to carry out electrocatalytic reduction of CO₂ to formate. Ion chromatography was used to quantify formate.

3.2.3 Electrokinetics

Linear sweep voltammetry results in a Tafel plot [31-34]. Fig. 7 is a Tafel plot obtained using molybdenum bronze film on conductive carbon in 0.5 M NaHCO₃ saturated with CO₂.

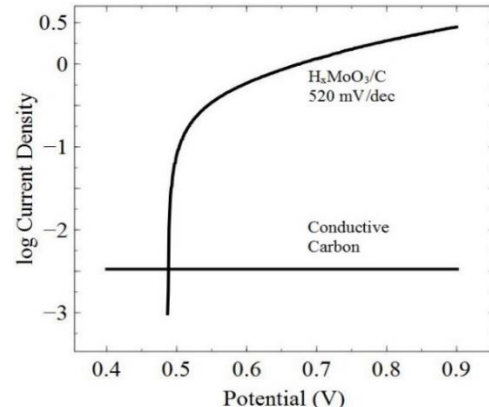


Fig. 7 Tafel plot using hydrogen bronze on conductive carbon reducing CO₂.

Electrokinetic analysis of these plots permits insight to the mechanism of reduction. The inverse of the potential range of interest in millivolts and logarithm of current results in a Tafel slope in units of mV/dec. Two consecutive electron transfer steps take place in production of formate. In the region of the greatest faradaic efficiency for formate the slope is 520 mV/dec. Nitrogen doped graphene quantum dots for reduction of carbon dioxide result in a slope of 489 mV/dec [34]. The theoretical Tafel slope for a one electron process is 118 mV/dec under standard conditions [35]. One reason for a Tafel slope higher than 118 mV/dec is due to adsorption and desorption rates of the reactants and products. Tafel slopes that approach 118 mV/dec but are less than 500 mV/dec indicate adsorption and desorption are faster but continue to be the rate determining step [14]. Tafel slopes are also dependent on film morphology. Slower electrodeposition times controlling current may result in more crystalline films and Tafel slopes in better agreement with the theoretical slope for one or two electron transfer reactions.

3.3 Electrochemical Reduction of Carbon Dioxide

3.3.1 Experimental Results

A 1,000 ppm standard of formate was diluted using 0.5 M NaHCO₃ to prepare standards for ion chromatography. Peak area was plotted with concentration and the slope of the linear plot (Fig. 8) was used to quantify ppm in triplicate trials to determine formate in ppm as well as error at

each applied potential. Table 3 shows the applied potential, amount of formate (ppm), charge in Coulombs and Faradaic efficiency. Fig. 9 is a plot of Faradaic efficiency and applied potential to the working electrode.

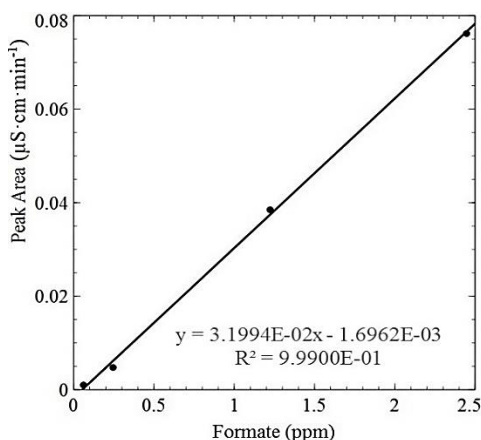


Fig. 8 Calibration for determination of formate

Table 3 The applied potential, amount of formate (ppm), charge and Faradaic efficiency for electrochemical reduction of carbon dioxide

Potential (V)	Formate (ppm)	Charge (Coulombs)	Faradaic efficiency (%)
-1.4	0.23	26.44	0.07
-1.2	0.11	11.886	0.08
-1.0	0.10	6.25	0.14
-0.8	0.15	1.599	0.78
-0.6	0.66	0.2961	1.85
-0.4	0.068	0.1219	5.03

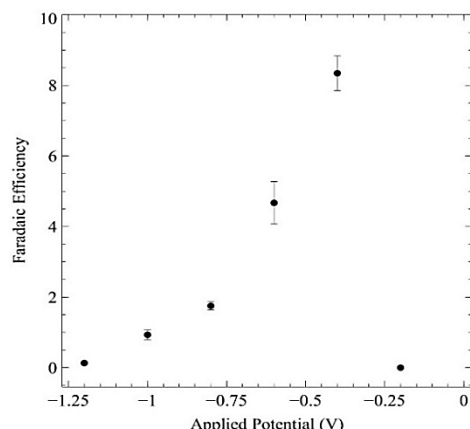


Fig. 9 Faradaic efficiency (%) plotted against applied potential

The highest amount of formate obtained required an applied potential of -1.4 V. However, this results in a greater charge causing the Faradaic efficiency to be very low, 0.07%.

In this work, the Faradaic efficiency is greatest at an applied potential of -0.4 V corresponding to an over potential of 0.2 V compared to the standard reduction potential of carbon dioxide to formate, -0.4 V [7]. The Faradaic efficiency in this work compared to other systems is low. However, the hydrogen molybdenum bronze films prepared in this work are novel, very simple, inexpensive, easy to prepare and can be used the same day. The plot of Faradaic efficiency vs. potential normally results in a volcano plot with a peak potential and maximum faradaic efficiency.

These results show that the hydrogen molybdenum bronze film is catalytic for reduction of carbon dioxide. A maximum amount of formate was obtained at -1.0 V (0.96 ppm). The reduction potential for CO₂ to formate vs the RHE at a pH of 8.3 is calculated to be +0.054 V [36]. An applied potential of -0.4 V vs the silver/silver chloride reference corresponds to +0.3 V vs the RHE. This potential is much more positive compared to use of palladium and platinum alloys deposited on carbon, -0.5 V vs the RHE [37]. Interestingly, formate dehydrogenase is known to contain molybdenum and tungsten active sites for reduction of CO₂ to formate [38]. Formate dehydrogenase was used as an electrocatalyst for reduction of CO₂ to formate. In a solution of 10 mM CO₂ and formate buffered to a pH of 8.0 the reduction potential was found to be approximately -0.45 V vs the SHE [39]. The reduction potential becomes more positive as the pH decreases from 8.0 to 6.0. A similar study using formate dehydrogenase at a pH of 6.5 resulted in a maximum FE for reduction of CO₂ to formate using an applied potential of -0.41 V vs. the

SHE [38]. In this work a maximum FE for formate was obtained at -0.4 V (-0.165 V vs SHE). This is more positive compared to use of formate dehydrogenase likely due to carrying out reduction of CO₂ at a pH of 8.3. This result indicates that the electrodeposited hydrogen molybdenum bronze films are likely capable of biomimicking formate dehydrogenase due to containing molybdenum as an active metal site for electrochemical reduction. In this work a maximum FE was obtained at -0.4 V (8.34%). Compared to Table 1, this result matches the lowest FE obtained using ruthenium electrocatalysts. Future strategies are aimed at improving the faradaic efficiency of electrodeposited hydrogen bronze films toward CO₂ reduction to formate. Headspace analysis of the electrochemical cell is critical to show that hydrogen bronze films electrodeposited on carbon paper may prevent CO poisoning.

4. Conclusion

Hydrogen molybdenum bronze films were prepared by electrodeposition techniques. Molybdenum powder was dissolved using hydrogen peroxide. Glass/ITO substrates were used to carry out bulk electrolysis of peroxymolybdcic acid from 100 to 1400 seconds resulting in reproducible blue hydrogen molybdenum bronze films ranging from approximately 200–500 μm in thickness. The inverse of film thickness vs. time was found to be a linear plot. Conductivity measurements of the film were found to be independent of thickness (3 Ω) which may be due to the narrow range of film thicknesses tested. Characterization of the films including X-ray photoelectron spectroscopy was carried out proving that molybdenum was in the film and that the color change was not due to the ITO substrate. X-Ray diffraction revealed the amorphous nature of the films most likely due to the presence of different peroxymolybdate species in solution. The films are not electrochromic and cathodic currents result in film dissolution into the bulk. The films were found to be catalytic toward the electrochemical reduction of carbon dioxide. Electrokinetic analysis using a Tafel plot revealed a slope comparable to other electrocatalysts for reduction of CO₂. Slower deposition time of the hydrogen bronze film may result in Tafel slope that is more comparable to one or two electron transfer processes. A maximum Faradaic efficiency of 8% was observed at -0.4 V or an over potential of only 0.2 V. While this is low, these films are inexpensive and simple to prepare. Future experiments will carry out electrodeposition of the bronze film at lower currents to determine if deposited films are more crystalline as evident by XRD. The expectation is that a more crystalline film will result in a lower Tafel slope. Bimetallic modification of the films are also planned to improve efficiency and selectivity for formate.

Funding and Acknowledgements

East Tennessee State University Office of Sponsored Research and Programs provided funding of the project. The authors also credit and thank those who characterized the films. Dr. Dwight Myers carried out X-ray diffraction of the films at East Central University. Greatly appreciated are conversations regarding the analysis of the films. Dr. Nicholas Materer performed XPS, and Dr. Toby Nelson measured film thickness and conductivity at Oklahoma State University.

References

- [1] Borgschulte, Andreas, Olga Sambalova, Renaud Delmelle, Sandra Jenatsch, Roland Hany, Frank Nüesch, Hydrogen reduction of molybdenum oxide at room temperature, *Sci. Rep.* 7 (2017) 40761:1–9.
- [2] Wan Danial Shahizuan, Yusarie Mohd, Influence of pH solution on the electrodeposition of tungsten oxide (WO₃) films onto indium tin oxide (ITO)-glass substrate, *Jour. Sci.Tech.* 4 (2012) 49–60.
- [3] K.J. Patel, C.J. Panchal, V.A. Kheraj, M.S. Desai, Growth, structural, electrical and optical properties of the thermally evaporated tungsten trioxide (WO₃) thin films, *Mater. Chem. Phys.* 114 (2009) 475–478.
- [4] Kadossov, B. Evgeni, Ahmad Razzaghi Soufiani, Allen W. Apblett, Nicholas F. Materer, Density-functional studies of hydrogen peroxide adsorption and dissociation on MoO₃(100) and H_{0.33}MoO₃(100) surfaces, *RSC Adv.* 5 (2015) 97755–97763.
- [5] M.A. Macêdo, L.H. Dall'antonio, B. Valla, M.A. Aegeerter, Electrochromic smart windows, *J. Non-Cryst. Solids* 147 (1992) 792–798.
- [6] Materer, F. Nicholas, Allen Apblett, Evgeni B. Kadossov, Kashif Rashid Khan, et al., The preparation and chemical reaction kinetics of tungsten bronze thin films and nitrobenzene with and without a catalyst, *Surf. Sci.* 648 (2016) 345–351.
- [7] Zhao, Huazhang, Yan Zhang, Bin Zhao, Yingyue Chang, Zhenshan Li, Electrochemical reduction of carbon dioxide in an MFC-MEC system with a layer-by-layer self-assembly carbon nanotube/cobalt phthalocyanine modified electrode, *Environ. Sci. Tech.* 46 (2012) 5198–5204.

[8] Liu, Yanming, Shuo Chen, Xie Quan, Hongtao Yu, Efficient electrochemical reduction of carbon dioxide to acetate on nitrogen-doped nanodiamond, *J. Am. Chem. Soc.* 137 (2015) 11631-11636.

[9] Min, Xiaoquan, Matthew W. Kanan, Pd-Catalyzed Electrohydrogenation of carbon dioxide to formate: High mass activity at low overpotential and identification of the deactivation pathway, *J. Am. Chem. Soc.* 137 (2015) 4701-4708.

[10] Klinkova, Anna, Phil De Luna, Cao-Thang Dinh, Oleksandr Voznyy, et al., Rational design of efficient palladium catalysts for electroreduction of carbon dioxide to formate, *ACS Catal.* 6 (2016) 8115-8120.

[11] Shinagawa, Tatsuya, Gastón O. Larrazábal, Antonio J. Martín, Frank Krumeich, Javier Pérez-Ramírez, Sulfur-modified copper catalysts for the electrochemical reduction of carbon dioxide to formate, *ACS Catal.* 8 (2018) 837-844.

[12] Tornow, E. Claire, Michael R. Thorson, Sichao Ma, Andrew A. Gewirth, Paul J.A. Kenis, Nitrogen-based catalysts for the electrochemical reduction of CO_2 to CO , *J. Am. Chem. Soc.* 134 (2012) 19520-19523.

[13] Wang, Riming, Xiaohui Sun, Samy Ould-Chikh, Dmitrii Osadchii, Fan Bai, Freek Kapteijn, Jorge Gascon, Metal-organic-framework-mediated nitrogen-doped carbon for CO_2 electrochemical reduction, *ACS Appl. Mater. Interf.* 10 (2018) 14751-14758.

[14] Hu, Xin-Ming, Halvor Høen Hval, Emil Tveden Bjerglund, Kirstine Junker Dalgaard, et al., Selective CO_2 reduction to CO in water using earth-abundant metal and nitrogen-doped carbon electrocatalysts, *ACS Catal.* 8 (2018) 6255-6264.

[15] Umeda, Minoru, Yuuki Niitsuma, Tom Horikawa, Shofu Matsuda, Masatoshi Osawa, Electrochemical reduction of CO_2 to Methane on platinum catalysts without overpotentials: strategies for improving conversion efficiency, *ACS Appl. Energy Mater.* 3 (2020) 1119-1127.

[16] Summers, P. David, Steven Leach, Karl W. Frese, The electrochemical reduction of aqueous carbon dioxide to methanol at molybdenum electrodes with low overpotentials, *J. Electroanal. Chem. Interf. Electrochem.* 205 (1986) 219-232.

[17] S. Ayyappan, C.N.R. Rao, A simple method of hydrogen insertion in transition metal oxides to obtain bronzes, *Mater. Res. Bull.* 30 (1995) 947-951.

[18] Y. Gui, D.J. Blackwood, Electrochromic enhancement of $\text{WO}_3\text{-TiO}_2$ composite films produced by electrochemical anodization, *J. Electrochem. Soc.* 161 (2014) E191-E201.

[19] T. Ressler, J. Wienold, R.E. Jentoft, Formation of Bronzes during temperature programmed reduction of MoO_3 with hydrogen-an in situ XRD and XAFS study, *Solid State Ionics* 141-142 (2001) 243-252.

[20] Pathan, M. Habib, Sun-Ki Min, Kwang-Deog Jung, Oh-Shim Joo, Electrosynthesis of molybdenum oxide thin films onto stainless substrates, *Electrochem. Commun.* 8 (2006) 273-278.

[21] P.K. Shen, J. Syed-Bokhari, A.C.C. Tseung, The performance of electrochromic tungsten trioxide films doped with cobalt or nickel, *J. Electrochem. Soc.* 138 (1990) 2778-2783.

[22] Pauporté, Thierry, A simplified method for WO_3 electrodeposition, *J. Electrochem. Soc.* 149 (2002) C539-C545.

[23] Kazusuke, Yamanaka, Electrodeposited films from aqueous tungstic acid-hydrogen peroxide solutions for electrochromic display devices, *Jap. J. Appl. Phys.* 26 (1987) 1884-1890.

[24] S.H. Baeck, T. Jaramillo, G.D. Stucky, E.W. Mcfarland, Controlled electrodeposition of nanoparticulate tungsten oxide, *Nano Lett.* 2 (2002) 831-834.

[25] V. Kublanovsky, O. Bersirova, Yu. Yapontseva, H. Cesiulis, E. Podlaha-Murphy, Cobalt-molybdenum-phosphorus alloys: Electroplating and corrosion properties, *Protect. Metal. Phys. Chem. Surf.* 45 (2009) 588-594.

[26] Y.J. Huang, H.H. Dai, W.S. Li, G.L. Li, D. Shu, H.Y. Chen, Electrodeposition preparation of $\text{Pt}-\text{H}_x\text{WO}_3$ composite and its catalytic activity toward oxygen reduction reaction, *J. Power Sour.* 184 (2008) 348-352.

[27] Kondrachova, Lilia, Benjamin P. Hahn, Ganesh Vijayaraghavan, Ryan D. Williams, Keith J. Stevenson, Cathodic electrodeposition of mixed molybdenum tungsten oxides from peroxy-poly(molybdate) solutions, *Langmuir* 22 (2006) 10490-10498.

[28] Taube, Fabian, Characterization of aqueous peroxy(molybdate)s with catalytic applicability, *Departmeant of Chemistry, Umea University, Sweden*, 2002, p.65

[29] Metrohm, Organic acid anions besides the standard anions separated on the Metrosep A Supp 16 - 250/4.0 column, http://partners.metrohm.com/GetDocument?action=get_dms_document&docid=696157 (Accessed on: 20.09.2017)

[30] McEvoy, M. Todd, Keith J. Stevenson, Electrochemical quartz crystal microbalance study of the electrodeposition mechanism of molybdenum oxide thin films from peroxy-poly(molybdate) solution, *Anal. Chim. Acta* 496 (2003) 39-51.

[31] T. Shinagawa, A.T. Garcia-Esparza, K. Takanabe, Insight on Tafel slopes from a microkinetic analysis of aqueous electrocatalysis for energy conversion, *Sci. Rep.* 5 (2015) 1-21.

[32] Kim, Seok Ki, Yin-Jia Zhang, Helen Bergstrom, Ronald Michalsky, Andrew Peterson, Understanding the low-overpotential production of CH_4 from CO_2 on Mo_2C catalysts, *ACS Catal.* 6 (2016) 2003-2013.

[33] Fang, Ya-Hui, Zhi-Pan Liu, Tafel kinetics of electrocatalytic reactions: From experiment to first-principles, *ACS Catal.* 4 (2014) 4364-4376.

[34] Wu, Jingjie, Sichao Ma, Jing Sun, Jake I. Gold, et al., A metal-free electrocatalyst for carbon dioxide reduction to multi-carbon hydrocarbons and oxygenates, *Nature Commun.* 7 (2016) 13869:1-6.

[35] Wang, Joseph, *Analytical electrochemistry*, Wiley-VCH, German, 2006.

[36] Ruud Kortlever, Jing Shen, Klaas Jan P. Schouten, Federico Calle-Vallejo, Marc T.M. Koper, Catalysts and reaction pathways for the electrochemical reduction of carbon dioxide, *J. Phys. Chem. Lett.* 6 (2015) 4073-4082.

[37] Ruud Kortlever, Ines Peters, Sander Koper, Marc T.M. Koper, Electrochemical CO_2 reduction to formic acid at low overpotential and with high faradaic efficiency on carbon-supported bimetallic Pd-Pt nanoparticles, *ACS Catal.* 5 (2015) 3916-3923.

[38] Torsten Reda, Caroline M. Plugge, Nerilie J. Abram, Judy Hirst, Reversible interconversion of carbon dioxide and formate by an electroactive enzyme, *Proc. Nat. Acad. Sci.* 105 (2008) 10654-10658.

[39] Bassegoda Arnaud, Christopher Madden, David W. Wakerley, Erwin Reisner, Judy Hirst, Reversible interconversion of CO_2 and formate by a molybdenum-containing formate dehydrogenase, *J. Am. Chem. Soc.* 136 (2014) 15473-15476.